

IAC-12-C1.9.7

ATTITUDE MOTION PLANNING FOR A SPIN STABILISED DISK SAIL

Craig Maclean

Advanced Space Concepts Laboratory, Glasgow, UK
 craig.maclean@strath.ac.uk

James Biggs

Advanced Space Concepts Laboratory, Glasgow, UK
 james.biggs@strath.ac.uk

While solar sails are capable of providing continuous low thrust propulsion the size and flexibility of the sail structure poses difficulties to their attitude control. Rapid slewing of the sail can cause excitation of structural modes, resulting in flexing and oscillation of the sail film and a subsequent loss of performance and decrease in controllability. Disk shaped solar sails are particularly flexible as they have no supporting structure and so these spacecraft must be spun around their major axis to stiffen the sail membrane via the centrifugal force. In addition to stiffening the structure this spin stabilisation also provides gyroscopic stiffness to disturbances, aiding the spacecraft in maintaining its desired attitude. A method is applied which generates smooth reference motions between arbitrary orientations for a spin-stabilised disk sail. The method minimises the sum square of the body rates of the spacecraft, therefore ensuring that the generated attitude slews are slow and smooth, while the spin stabilisation provides gyroscopic stiffness to disturbances. An application of Pontryagin's maximum principle yields an optimal Hamiltonian which is completely solvable in closed form. The resulting analytical expressions are a function of several free parameters enabling parametric optimisation to be used to provide reference motions which match prescribed boundary conditions on the initial and final configurations. The generated reference motions are utilised in the repointing of a 70m radius spin-stabilised disk solar sail in a heliocentric orbit, with the aim of assessing the feasibility of the motion planning method in terms of the control torques required to track the motions.

Key words: solar sail, motion planning, geometric control

I. NOMENCLATURE

a_c	Characteristic acceleration of solar sail (m/s^2)	\bar{r}_{mp}	Centre of mass to centre of pressure vector (m)
\bar{a}_{SRP}	Acceleration due to solar radiation pressure (m/s^2)	r_y, r_z	Position of sliding masses along y and z body axes (m)
A_1, A_2, A_3	Basis of the Lie algebra on $su(2)$	$\hat{R}, \hat{T}, \hat{N}$	Basis of the RTN reference frame
A_r	Reflective area (m)	$\bar{R}(t)$	Kinematics on $SU(2)$
\bar{F}_{SRP}	Solar radiation pressure force (N)	R_{ob}	Rotation matrix from RTN to body frame
$\hat{i}, \hat{j}, \hat{k}$	Basis of the body reference frame	v	Spin rate of spacecraft (rad/s)
$\hat{I}, \hat{J}, \hat{K}$	Basis of the heliocentric ecliptic reference frame	α	Cone angle ($degrees$)
J_1, J_2, J_3	Principal moments of inertia of spacecraft (kgm^2)	δ	Clock angle ($degrees$)
m_a	Attached mass (excluding sail) (kg)	σ_a	Attached mass assembly loading (kg/m^2)
m_s	Sail mass (kg)	σ_s	Sail assembly loading (kg/m^2)
\hat{n}	Sail normal unit vector	$\bar{\omega}_{bi}$	Inertially referenced body rates (rad/s)
\bar{N}	Control torques (N)	$\bar{\omega}_{bo}$	RTN referenced body rates (rad/s)
P	Mean solar radiation pressure at 1AU (N/m^2)	$\bar{\omega}_{oi(b)}$	Orbital rate with respect to inertial frame, expressed on body reference frame components (rad/s)
\bar{q}	Quaternions of body frame with respect to RTN frame	$\bar{\omega}_e$	Angular velocity error (rad/s)
\bar{q}_e	Quaternion error		
\bar{r}	Radial vector from Sun to spacecraft (m)		

II. INTRODUCTION

While solar sailing as a concept has existed since the early part of the 20th century, it is only recently that advances in materials research has enabled practical solar

sails to be designed and built. Solar sailing has gathered considerable interest as it has the ability to provide continuous, low thrust propulsion without the need for propellant, enabling mission lifetimes to be extended and the creation of previously unattainable orbits. Examples of missions enabled by solar sailing include the GeoSail mission [1, 2], the Solar-Polar Orbiter [3] and the Interstellar Heliopause Mission [4]. Yet while a large body of work has been carried out into the orbital dynamics of solar sails, the practical attitude control required to achieve these missions has been somewhat neglected with most papers simply deriving the instantaneous changes in sail attitude necessary to achieve a certain trajectory. However solar sails are flexible structures with large moments of inertia which poses significant problems to their attitude control.

The flexible nature of solar sails means that manoeuvre times are necessarily large to avoid excessive excitation of the sail structure due to large or impulsive control torques. Moreover conventional actuators such as reaction wheels are often impractical for solar sail attitude control. Solar sails can be subjected to large gravity gradient torques meaning that reaction wheels quickly saturate in planet centred orbits [5], unless the orbit is carefully chosen [6]. Furthermore reaction wheel size increases with sail size and may become undesirably high for large solar sails, with the added mass an impediment to their launch and operation. In addition for missions far from Earth magnetorquers cannot be used for desaturation, meaning cold gas or electric thrusters for example would have to be used. However thrusters are undesirable for solar sail attitude control as fast impulsive torques will excite the sail structure and the propellant ejected may contaminate the sail. Thrusters also have a finite supply of propellant which may reduce the operational mission lifetime.

As a result of the difficulties with conventional actuators, several new methods of actuating solar sails have been proposed. Wie, who carried out the first large body of work on the attitude control of solar sails in Earth centred orbits [5, 7], examined the use of controllable booms to change the offset between the centre of pressure and centre of mass of the spacecraft and so produce the control torques. The torques produced are continuous, lessening the impact on the sail membrane, and no propellant is expended. However this method posed considerable engineering challenges related to the structure of the control booms, with boom size increasing with solar sail size. Controllable sliding masses along sail struts have also been studied as a means of producing control torques via a changing centre of mass centre of pressure offset [8]. In these cases the dynamics of the system were linearised and solved to give the required euler angles, which were then tracked using a proportional-integral-derivative (PID) controller. The sliding ballast method was used to produce the attitude control necessary to implement a transfer to Mercury in [9], with inverse control used to derive the position of the masses necessary to produce the required torques. The sliding bal-

last method was extended by [10, 11] who used both a feedforward controller based on the eigenaxis theorem to compute the attitude manoeuvre and a feedback controller to account for the position and angular velocity errors. The authors in [12] utilised the sliding ballast method for quaternion feedback repointing in addition to BDOT control for detumbling of a small sail in Earth orbit. Wie combined the sliding ballast method with tip mounted pulsed plasma thrusters (PPTs), with the PPTs employed to control the spin rate [8]. In this paper the desired euler angles were again found and tracked using PID control.

Control vanes and electrochromic surfaces have also been proposed as actuation methods for solar sails. The use of control vanes, small reflective surfaces located at the sail extremities, was described in [8, 13] and tested in simulation. However control vanes require mechanical actuation to control their articulation, adding extra complexity. Funase [14] detailed a system, included on the spinning IKAROS sail, to provide two-axis stabilisation by switching the reflectivity of electrochromic sections. Switching the reflectivity between two different states changes the torque due to solar radiation pressure (SRP) acting on the sail, and can be regulated to produce the required control torques.

While challenges to their implementation remain, sliding ballast masses and electrochromic control seem to be the most feasible methods for solar sail actuation at present as neither utilise propellant mass and both provide continuous control torques which should lessen the impact on the sail structure. Therefore, in this paper we look to assess the feasibility of using actuators that can apply a continuous torque and see if the torque requirement is within the range of current solar sail technologies such as sliding ballast masses and electrochromic control.

This paper tackles the attitude control of a spin stabilised solar sail using a motion planning method, derived through the framework of geometric control theory, which minimises the body rates of the spacecraft. With spin stabilisation the entire spacecraft rotates around its own pointing axis using the gyroscopic effect [15]. Spin stabilisation is vital for disk type solar sails as they generally do not have any supporting structure and so are very susceptible to flexing. These sails rely on the stiffening effect of the centrifugal force brought about by the spin [13]. Therefore in order to reduce the effect on the structure of the sail during slewing, it may be beneficial to limit the body rates around the non-spinning axes.

The design of reference motions subject to constraints, such as limiting the body rates, is often formulated and solved in the context of constrained optimal control problems. These type of problems generally define the attitude kinematics and the Euler equations as equality constraints, with the performance index a function of control torques and/or time subject to prescribed boundary conditions and inequality constraints such as bounding the instantaneous torque [16, 17, 18]. Other optimisation approaches such as the locally op-

timal Euler Lagrange approach of calculus of variations were used to solve problems such as time-optimal attitude control [19] and the minimum fuel problem for a fixed time horizon [20]. These local methods have the added complexity of numerically solving two point boundary value problems onboard the spacecraft. The Hamilton-Jacobi-Bellman (HJB) approach from dynamic programming is globally stabilising, but is numerically intractable. Solving it off-line is possible numerically, [21] but the global optimal solution is only approximated up to a certain order, which cannot be too high for practical implementation.

In this paper an application of the method outlined in [22] is applied to the motion planning in order to try to improve the control of a spinning disk solar sail. Using the mechanisms of geometric control theory, the kinematics of the spacecraft are written in terms of the Lie algebra on $SU(2)$ and an optimal Hamiltonian derived via an application of Pontryagin's maximum principle. This leads to the derivation of analytical expressions for the optimal angular velocities and the time evolution of the quaternions. These analytical expressions can then be parametrically optimised to meet boundary conditions imposed on the final pointing direction. The motion planning method is illustrated in simulation for a 70m radius spinning disk sail in a heliocentric orbit. References are tracked using a conventional quaternion feedback controller and assuming ideal actuators which are capable of providing a continuous torque. This will provide an initial analysis of the required torques to perform certain motions which will give an indication of the type of actuators which could feasibly be used. It is shown that the method can be used to perform slews typical of an inclination change manoeuvre for a solar sail in a heliocentric orbit.

This paper serves as a first step in designing attitude manoeuvres for solar sails which initially concentrates on minimising body rates to avoid excitation. The extension to a multi-objective function including torque will be considered elsewhere.

III. MODELS

While the solar sail is in reality a flexible structure, in this paper the simplifying assumption is made that the spacecraft can be treated as a rigid disk. This assumption is feasible as the attitude of the sail disk will be moving at such a slow rate that the flexible structure will not be excited. The general equations describing the attitude control problem are then that of a rigid body with external forces describing the effect of the actuators and perturbations.

Reference Frame Definitions

The spacecraft under consideration is in orbit around the Sun. The centre of the Sun is chosen as the origin of a heliocentric ecliptic reference system with basis vectors $\hat{I}, \hat{J}, \hat{K}$. As in [23], the X and Y axes lie in the ecliptic plane towards the vernal equinox and winter solstice positions of the Earth respectively, with the Z-

axis completing the orthonormal reference frame. The co-ordinate system is shown in Figure 1.

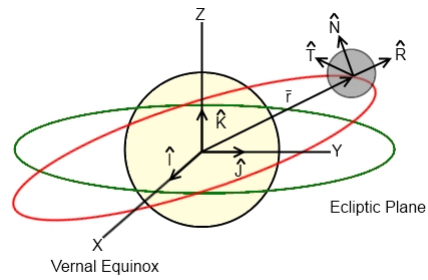


Figure 1: Heliocentric ecliptic and RTN co-ordinate systems.

Also shown in Figure 1 is the Radial-Transverse-Normal (RTN) reference frame used to describe the orbit of the spacecraft. In this reference frame \hat{R} is parallel with the radial vector, \hat{N} is parallel with the orbit normal and \hat{T} completes the orthonormal frame. A body fixed reference frame (BRF) with basis $\hat{i}, \hat{j}, \hat{k}$ is rigidly attached to the centre of mass of the spacecraft. The body and RTN frames are coincident when the sail attitude angles (cone angle α and clock angle δ) are zero. The body rates $\bar{\omega}_{bo} = [\omega_{1bo} \ \omega_{2bo} \ \omega_{3bo}]^T$ describe the rotation of the body frame with respect to the orbit frame.

Finally, a non-spinning frame (NSF) which is fixed to the x-axis of the body frame but does not spin is employed. Since the spacecraft is symmetric, only the direction of the spin axis is of importance (for pointing of the thrust vector.) Therefore the non-spinning frame is employed to show that the spin-axis of the sail has achieved a certain orientation with respect to the orbit frame when the angular velocities around the non-spinning axes are brought to zero.

Kinematic Model

The attitude kinematics of the spacecraft in the body frame with respect to the RTN orbit frame can be parameterised using quaternions:

$$\frac{d\bar{q}}{dt} = \frac{1}{2}\Omega\bar{q} \quad (1)$$

Where $\bar{q} = [q_0 \ q_1 \ q_2 \ q_3]^T$ denotes the quaternions which represent the attitude of the spacecraft in the body frame with respect to an RTN orbit frame, and $\frac{d\bar{q}}{dt}$ their rate of change. Note that the subscript bo (body with respect to orbit) is omitted in the description of the quaternions and unless otherwise stated the quaternions represent the attitude of the body frame with respect to the orbit frame. The skew symmetric matrix Ω is given by:

$$\Omega = \begin{pmatrix} 0 & -\omega_{1bo} & -\omega_{2bo} & -\omega_{3bo} \\ \omega_{1bo} & 0 & \omega_{3bo} & -\omega_{2bo} \\ \omega_{2bo} & -\omega_{3bo} & 0 & \omega_{1bo} \\ \omega_{3bo} & \omega_{2bo} & -\omega_{1bo} & 0 \end{pmatrix} \quad (2)$$

The quaternions must satisfy the constraint $q_0^2 + q_1^2 + q_2^2 + q_3^2 = 1$. The quaternion differential equations are used as they do not suffer from problems with singularities or imaginary numbers. This representation is equivalent to the kinematic matrix representation on $SU(2)$:

$$\frac{d\bar{R}(t)}{dt} = \bar{R}(t)(\omega_{1bo}A_1 + \omega_{2bo}A_2 + \omega_{3bo}A_3) \quad (3)$$

where $\bar{R}(t) \in SU(2)$ represents the spacecrafts orientation, A_1, A_2, A_3 form a basis for the Lie algebra $\mathfrak{su}(2)$ of the Lie group $SU(2)$:

$$\begin{aligned} A_1 &= \frac{1}{2} \begin{pmatrix} i & 0 \\ 0 & -i \end{pmatrix} \\ A_2 &= \frac{1}{2} \begin{pmatrix} 0 & 1 \\ -1 & 0 \end{pmatrix} \\ A_3 &= \frac{1}{2} \begin{pmatrix} 0 & i \\ i & 0 \end{pmatrix} \end{aligned} \quad (4)$$

where i is an imaginary number and the Lie algebra's commutator defined by $[X, Y] = YX - XY$ called the Lie bracket with $X, Y \in \mathfrak{su}(2)$ such that $[A_1, A_2] = A_3$, $[A_2, A_3] = A_1$ and $[A_1, A_3] = -A_2$ where $\bar{R}(t) \in SU(2)$ is of the form:

$$\bar{R}(t) = \begin{pmatrix} z_1 & z_2 \\ -\bar{z}_2 & \bar{z}_1 \end{pmatrix} \quad (5)$$

with $z_1, z_2 \in \mathbb{C}$ and \bar{z}_1, \bar{z}_2 their complex conjugates such that $|z_1|^2 + |z_2|^2 = 1$. Physically the basis A_1, A_2, A_3 describe the infinitesimal motion of the spacecraft in the roll, pitch and yaw directions respectively. Furthermore, the two sets of kinematic equations (1) and (3) are equivalent with the isomorphism $F : SU(2) \leftrightarrow H$:

$$F : \begin{pmatrix} z_1 & z_2 \\ -\bar{z}_2 & \bar{z}_1 \end{pmatrix} \leftrightarrow \mathbf{z}_1 + \mathbf{z}_2 \cdot \mathbf{j} = q_0\mathbf{e} + q_1\mathbf{i} + q_2\mathbf{j} + q_3\mathbf{k} \quad (6)$$

defining the coordinate change and where the complex numbers $z_1 = q_0 + iq_1, z_2 = q_2 + iq_3$ are regarded in their quaternion form $\mathbf{z}_1 = q_0\mathbf{e} + q_1\mathbf{i}, \mathbf{z}_2 = q_2\mathbf{e} + q_3\mathbf{i}$ subject to the usual quaternionic multiplication. For more details of this isomorphism see [24] pp. 169-171.

Dynamic Model

Euler's rotational equations of motion for a rigid spacecraft are defined as:

$$J \cdot \dot{\bar{\omega}}_{bi} + \bar{\omega}_{bi} \times J \cdot \bar{\omega}_{bi} = \bar{N} \quad (7)$$

Where J denotes the moment of inertia matrix of the spacecraft, $\bar{\omega}_{bi}$ and $\dot{\bar{\omega}}_{bi}$ the angular velocity and angular acceleration vectors of the spacecraft in the inertial frame and $\bar{N} = [N_1 \ N_2 \ N_3]^T$ the external torques. Since no disturbance torques are modelled, the external torques are simply the control torques. Assuming that the body frame originates from the spacecraft centre of

mass and is coincident with the principal axis of the spacecraft, Euler's equations reduce to:

$$\begin{aligned} \dot{\omega}_{bi1} &= \frac{N_1 + (J_2 - J_3)\omega_{bi2}\omega_{bi3}}{J_1} \\ \dot{\omega}_{bi2} &= \frac{N_2 + (J_3 - J_1)\omega_{bi3}\omega_{bi1}}{J_2} \\ \dot{\omega}_{bi3} &= \frac{N_3 + (J_1 - J_2)\omega_{bi1}\omega_{bi2}}{J_3} \end{aligned} \quad (8)$$

Where J_1, J_2 and J_3 are the principal moments of inertia of the spacecraft. The absolute angular velocity of the spacecraft in the inertial frame, ω_{bi} is given by:

$$\bar{\omega}_{bi} = \bar{\omega}_{bo} + \bar{\omega}_{oi(b)} \quad (9)$$

where $\bar{\omega}_{oi(b)}$ is the angular velocity of the orbital frame with respect to the inertial frame, expressed in body frame components. This component can be computed via:

$$\bar{\omega}_{oi(b)} = R_{ob}\bar{\omega}_{oi} \quad (10)$$

where R_{ob} is the rotation matrix from the orbit frame to the body frame in quaternion components with elements:

$$\begin{aligned} R_{11ob} &= 1 - 2(q_2^2 + q_3^2) \\ R_{12ob} &= 2(q_1q_2 + q_3q_0) \\ R_{13ob} &= 2(q_1q_3 - q_2q_0) \\ R_{21ob} &= 2(q_1q_2 - q_3q_0) \\ R_{22ob} &= 1 - 2(q_1^2 + q_3^2) \\ R_{23ob} &= 2(q_3q_2 + q_1q_0) \\ R_{31ob} &= 2(q_1q_3 + q_2q_0) \\ R_{32ob} &= 2(q_2q_3 - q_1q_0) \\ R_{33ob} &= 1 - 2(q_1^2 + q_2^2) \end{aligned} \quad (11)$$

The quaternions which describe the attitude of the non-spinning frame with respect to the orbit frame can be found from the quaternions relating the body frame to the orbit frame, and the quaternion multiplication rule in matrix form [7]:

$$\bar{q}_f = \begin{bmatrix} q_{0r} & q_{1r} & q_{2r} & q_{3r} \\ -q_{1r} & q_{0r} & q_{3r} & -q_{2r} \\ -q_{2r} & -q_{3r} & q_{0r} & q_{1r} \\ -q_{3r} & q_{2r} & -q_{1r} & q_{0r} \end{bmatrix} \bar{q}_i \quad (12)$$

where $\bar{q}_r = [q_{0r} \ q_{1r} \ q_{2r} \ q_{3r}]^T$ are the quaternions specifying the rotation, \bar{q}_i the quaternions before the rotation is applied and \bar{q}_f the quaternions resulting from the rotation.

In the case of the rotation from the body frame to the non-spinning frame $\bar{q}_r = [\cos \gamma/2 \ -\sin \gamma/2 \ 0 \ 0]^T$ where $\gamma = vt$ and v is the spacecraft spin rate, \bar{q}_f are the quaternions in the non-spinning frame and \bar{q}_i are the quaternions of the body frame with respect to the orbit frame.

Solar Sail Properties

Table 1 lists some of the properties of the solar sail under consideration. Assuming that the payload is a point mass located at the centre of the sail, and that no

Sail radius	70 m
Sail characteristic acceleration	$5 \times 10^{-4} m/s^2$
Total assembly loading	$0.01824 kg/m^2$
Sail assembly loading	$5 \times 10^{-3} kg/m^2$
Total assembly mass	280.77 kg
Sail mass	76.97 kg

Table 1: Solar sail properties

offset exists between the centre of mass and centre of pressure, we calculate the principal moments of inertia of the spacecraft to be $J_1 = 188.65 \times 10^3 kgm^2$, $J_2 = J_3 = 94.325 \times 10^3 kgm^2$.

Solar Radiation Pressure Model

The sail is assumed to be ideal. From [13] the acceleration due to solar radiation pressure, \bar{a}_{SRP} , for an ideal sail is given by:

$$\bar{a}_{SRP} = F_0(\hat{r} \cdot \hat{n})^2 \hat{n} \quad (13)$$

where \bar{r} is the radial vector from the Sun and \hat{r} the unit vector, \hat{n} is the sail normal unit vector (corresponding to [1 0 0] in the body frame), and where:

$$F_0 = \left(\frac{r_{AU}}{|\bar{r}|}\right)^2 a_c \quad (14)$$

with r_{AU} the mean distance from the Earth to the Sun (1AU) and a_c the sail characteristic acceleration. The characteristic acceleration of an ideal sail is given by:

$$a_c = \frac{2P}{\sigma_s + \sigma_a} \quad (15)$$

where $P = 4.563 \times 10^{-6} N/m^2$ is the nominal solar radiation pressure constant at 1AU from the Sun. The sail and attached mass assembly loadings are given as $\sigma_s = \frac{m_s}{A_r}$ and $\sigma_a = \frac{m_a}{A_r}$ respectively, where m_s and m_a are the masses of the sail and attached mass and A_r is the reflective area.

IV. DERIVATION OF REFERENCE MOTIONS

In this section a summary of the method in [22] is given which enables the derivation of the reference motions. The formulation of the motion planning method is described in the context of a constrained functional optimisation problem that includes equality constraints and a performance index (an integral function of the angular velocities). This formulation ensures smooth and feasible motions are defined and enable the derivation of analytic solutions in closed form. This renders a class of feasible curves subject to the equality constraint that satisfy the necessary conditions for optimality. This analytic form essentially reduces the original constrained functional optimisation problem to an unconstrained parameter optimisation problem where the

parameters are chosen to match the boundary conditions. The motion planning problem is defined by the kinematic constraint (equality constraint):

$$\frac{d\bar{R}(t)}{dt} = \bar{R}(t)(vA_1 + \omega_{2bo}A_2 + \omega_{3bo}A_3) \quad (16)$$

where the spacecraft is constrained to spin around its major axis at a constant rate $\omega_{1bo} = v$. Amongst all admissible motions of (16) we seek solutions that minimise the functional $l(\bar{R}(t)) = \int_0^T \left\langle \frac{d\bar{R}(t)}{dt}, \frac{d\bar{R}(t)}{dt} \right\rangle dt$ between the given boundary conditions $\bar{R}(0) = \bar{R}_0$ and $\bar{R}(T) = \bar{R}_T$ where T is a fixed-terminal time and $\langle \cdot, \cdot \rangle = -\frac{1}{2} \text{trace}(\cdot, \cdot)$ is the trace form. As the trace form is left (respectively right) invariant this is equivalent to minimising $l(\bar{R}(t)) = \int_0^T \left\langle \bar{R}(t)^{-1} \frac{d\bar{R}(t)}{dt}, \bar{R}(t)^{-1} \frac{d\bar{R}(t)}{dt} \right\rangle dt$ and from (16) it follows that $l(\bar{R}(t)) = \frac{1}{2} \int_0^T v^2 + \omega_{2bo}^2 + \omega_{3bo}^2 dt$. As v is constant on the fixed-time interval T this is equivalent to minimising the performance index:

$$f_0 = \frac{1}{2} \int_0^T \omega_{2bo}^2 + \omega_{3bo}^2 dt \quad (17)$$

This initial cost function is chosen as it (i) ensures smooth motions (ii) minimises the integral of angular velocities on the unconstrained axes which avoids the system accumulating more angular velocity than needed (iii) avoids dangerously fast slew rates which could excite the sail membrane, while making sure that the final attitude is specified (not at rest in final time but with small bounded final velocity) and (iv) allows the construction of the optimal motions in closed form using the framework of geometric control theory:

Lemma 1. *The class of reference motions that minimise the cost function (17) subject to the equality constraint (16) are defined by :*

$$\begin{aligned} \omega_{2bo}^* &= \zeta \sin((v+c)t + \beta) \\ \omega_{3bo}^* &= \zeta \cos((v+c)t + \beta) \end{aligned} \quad (18)$$

$$\begin{aligned} q_0^* &= \cos\left(\frac{1}{2}t(c+v)\right) \cos\left(\frac{Kt}{2}\right) + \frac{c}{K} \sin\left(\frac{1}{2}t(c+v)\right) \sin\left(\frac{Kt}{2}\right) \\ q_1^* &= \sin\left(\frac{1}{2}t(c+v)\right) \cos\left(\frac{Kt}{2}\right) - \frac{c}{K} \cos\left(\frac{1}{2}t(c+v)\right) \sin\left(\frac{Kt}{2}\right) \\ q_2^* &= \pm \frac{\zeta}{K} \sin\left(\frac{c+v}{2}t + \beta\right) \sin\left(\frac{Kt}{2}\right) \\ q_3^* &= \pm \frac{\zeta}{K} \cos\left(\frac{c+v}{2}t + \beta\right) \sin\left(\frac{Kt}{2}\right) \end{aligned} \quad (19)$$

where $\omega_{1bo}^* = v$, ω_{2bo}^* , ω_{3bo}^* are the optimal angular velocities and q_0^* , q_1^* , q_2^* , q_3^* the corresponding quaternion components subject to the given boundary conditions $\bar{q}(0) = \bar{q}_i = [1 \ 0 \ 0 \ 0]^T$ and $\bar{q}(T) = \bar{q}_f$ and where ζ, c, β are parameters available for optimisation, v is the given spinning angular velocity and $K = \sqrt{c^2 + \zeta^2}$ is a constant.

For proof, see reference [22]. This defines analytically a subset of admissible smooth motions expressed

in terms of several free parameters v, ζ, c, β (18,19). This initial constrained optimal control problem defined amongst all admissible curves has been reduced to a class of analytically defined feasible curves. This essentially reduces the motion planning problem to an unconstrained parameter optimisation problem.

The problem now is to choose the free parameters ζ, c, β such that the boundary conditions are matched at the terminal time $t = T$ (they are not included in the original performance index). In order to match a prescribed final pointing direction $\bar{q}_f = [q_{0f} \ q_{1f} \ q_{2f} \ q_{3f}]^T$ at the terminal time $t = T$ to high-precision the available parameters can be optimised to minimise the performance index:

$$\min_{\zeta, c, \beta} \{ (q_0 - q_{0f})^2 + (q_1 - q_{1f})^2 + (q_2 - q_{2f})^2 + (q_3 - q_{3f})^2 \}_{t=T} \quad (20)$$

The result is a set of optimal values of the free parameters ζ^*, c^*, β^* which can be input into (18) and (19) to give the optimal angular velocities and quaternions for the manoeuvre to $\bar{q}_f = [q_{0f} \ q_{1f} \ q_{2f} \ q_{3f}]^T$ in the time $t = T$. The analytical results can then be validated by comparison with the quaternions resulting from the numerical integration using the optimal angular velocities.

Note that the cost (20) only includes pointing error and not torque, so resulting motions will not be torque optimal. If the resulting torques are too high a function can be used as in [22] to reduce the torques required to track the motions, at the expense of increased error in the pointing direction.

V. APPLICATION TO A SPINNING DISK SAIL

The method described above was applied to the re-pointing of a spin stabilised disk solar sail in a heliocentric orbit. The semi-major axis of the orbit was chosen to be $0.24AU$, with all other orbital elements chosen to be zero at $t = 0$. A spin rate of $v = 0.0209rad/s$ was chosen as in [13]. Two example manoeuvres will now be shown. In each case the sail starts at the initial quaternion $\bar{q}_i = [1 \ 0 \ 0 \ 0]^T$, corresponding to cone and clock angles of $\alpha = \delta = 0^\circ$.

The desired cone and clock angles in each case can be converted to quaternions by utilising the quaternion multiplication rule (12) to rotate the initial quaternion in the body frame \bar{q}_i first by an angle $-\delta$ and then by $-\alpha$. These quaternions were then entered into the motion planner to generate the required reference motions. A conventional quaternion feedback controller is used to track the reference motions:

$$\bar{u}(t) = -C_1 \bar{q}_e - C_2 \bar{\omega}_e \quad (21)$$

where C_1, C_2 are gains and:

$$\bar{q}_e = \begin{bmatrix} q_{0f} & q_{1f} & q_{2f} & q_{3f} \\ -q_{1f} & q_{0f} & q_{3f} & -q_{2f} \\ -q_{2f} & -q_{3f} & q_{0f} & q_{1f} \\ -q_{3f} & q_{2f} & -q_{1f} & q_{0f} \end{bmatrix} \bar{q} \quad (22)$$

and $\bar{\omega}_e = \bar{\omega}_\alpha - \bar{\omega}_d$ is the error between the actual and desired angular velocities. Only the vector part of the

error quaternion \bar{q}_e (i.e. q_{1e}, q_{2e}, q_{3e}) is used in tracking. Since the method is not inherently rest-to-rest, in the final 2% of the manoeuvre the desired angular velocities in the non-spinning axes are switched to zero. The spacecraft was actuated using ideal thrusters around the two non-spinning axes. The manoeuvre time was chosen to be $1.01 \times 10^4 seconds$.

Manoeuvre A

In this case the sail is reorientated to a cone angle $\alpha = 35^\circ$ and clock angle $\delta = 0^\circ$ ($\bar{q}_f = [\cos 7\pi/72 \ 0 \ -\sin 7\pi/72 \ 0]^T$), corresponding to the attitude necessary for the initial stage of an inclination change manoeuvre. The results are shown in Figures 2, 3 and 4.

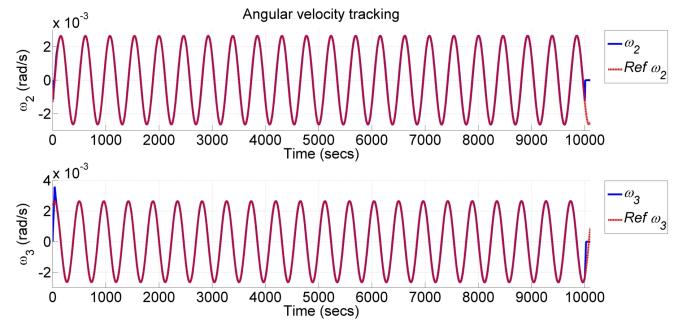


Figure 2: Angular velocity tracks for Manoeuvre A.

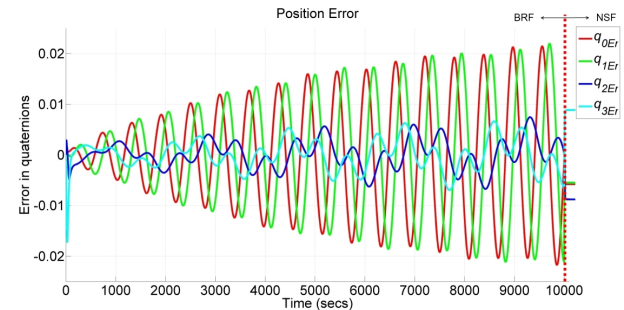


Figure 3: Error between actual and desired quaternions for Manoeuvre A. The dotted line marks the transition from the body reference frame (BRF) to the non-spinning frame (NSF).

Note that in Figure 3 the error in the quaternions q_{Er} is defined as the difference between the actual and desired quaternions at each time-step, and should not be confused with the quaternion error defined in (22). The sail reaches the desired attitude of the body frame with respect to the orbit frame in 9.99×10^3 seconds, before the control is switched to bring the spacecraft to a state of pure spin. After the switch in reference, the non-spinning reference frame is used to describe the attitude (shown as the dotted vertical line in Figure 3) and the error in the quaternions reaches a constant value, indicating the point at which a fixed attitude of

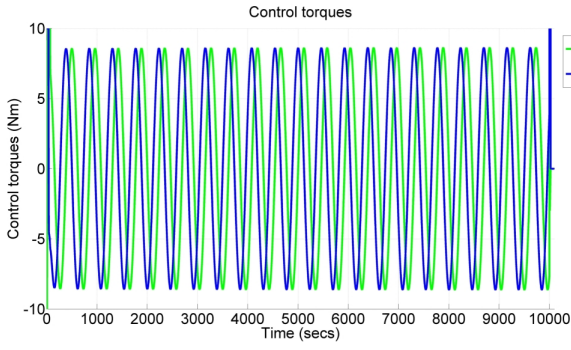


Figure 4: Control torques for Manoeuvre A.

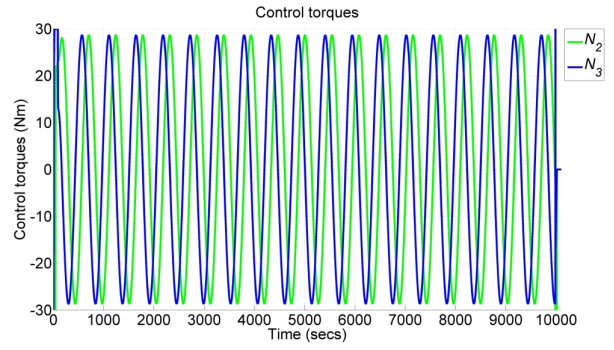


Figure 7: Control torques for Manoeuvre B.

the non-spinning frame with respect to the orbit frame has been reached.

Manoeuvre B

In this case the sail was reorientated to a cone angle $\alpha = 35^\circ$ and clock angle $\delta = 180^\circ$ ($\bar{q}_f = [0 \quad -\cos 7\pi/72 \quad 0 \quad \sin 7\pi/72]^T$). The results are shown in Figures 5, 6 and 7.

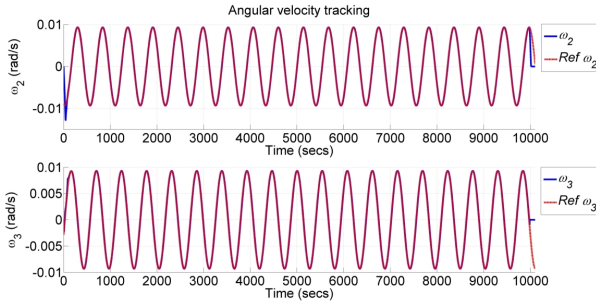


Figure 5: Angular velocity tracks for Manoeuvre B.

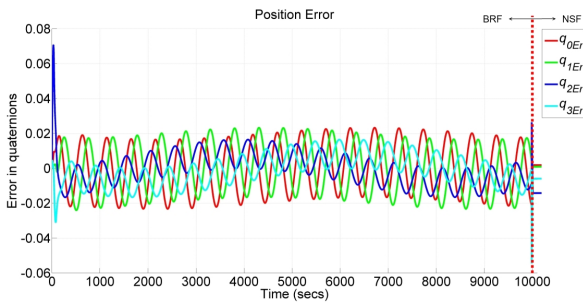


Figure 6: Error between actual and desired quaternions for Manoeuvre B. The dotted line marks the transition from the body reference frame (BRF) to the non-spinning frame (NSF).

VI. DISCUSSION

In the previous section the motion planning method was applied to the reorientation of a simple spinning

disk sail, enabling the sail to achieve a desired attitude without despining. However from Figures 4 and 7, the required torques are relatively high, of the order $10^1 Nm$. This is due to a combination of the moments of inertia of the solar sail under consideration being particularly high (of the order $10^5 kgm^2$), and the gyroscopic effect of the spinning sail, meaning that large control torques are required to change the sail attitude. Assuming that there is no offset in the x -axes, the available torques \bar{N} in the y and z body axes due to an offset between the centre of mass and centre of pressure can be found from:

$$\bar{N} = 0\hat{i} + (r_{mpz}F_{SRPx})\hat{j} - (r_{mpy}F_{SRPx})\hat{k} \quad (23)$$

where r_{mpy}, r_{mpz} are components of the centre of mass to centre of pressure vector \bar{r}_{mp} , F_{SRPx} is the x -component of the SRP force (\bar{F}_{SRP}) and \hat{j}, \hat{k} are unit vectors of the body frame. From simulation, the acceleration due to SRP in the x -axis at a distance of $0.24AU$ from the Sun reached a peak value of $0.0087m/s^2$. From [7] and [12], the conventionally assumed maximum centre of mass centre of pressure offset lies in the range $0.25 - 0.6\%$ of the characteristic length of the sail. For the $140m$ diameter sail considered here, this gives $\bar{r}_{mp} = [0 \quad 0.84 \quad 0.84]^T m$. Then, for a spacecraft mass of $280.77 kg$, $F_{srpx} = 2.44 N$ and from (23), the maximum torque available due to the centre of mass centre of pressure offset is $N_{max} = [0 \quad 2.05 \quad 2.05]^T Nm$. Manoeuvres A and B clearly violate this torque limit. Therefore the references from the motion planning method in this paper cannot be tracked using the sliding ballast method using an offset of $0.25 - 0.6\%$ of the characteristic length of the sail. From (23), an offset of $\bar{r}_{mp} = [0 \quad 12.3 \quad 12.3]^T m$ (8.8% of sail diameter) is required to produce a torque of $30Nm$ (the maximum torque in Manoeuvres A and B). Considering a system with two translating masses along the y and z body axes, with each mass equal to half the attached mass of the above sail ($101.9 kg$), the distance the masses would require to move can be found from pg. 791 of [7]:

$$\bar{r}_c = \frac{m_a/2}{m_s + m_a} (0\hat{i} + r_y\hat{j} + r_z\hat{k}) \quad (24)$$

Solving for r_y and r_z , the position of the masses along

the y and z body axes, leads to $r_y = r_z = 33.9m$.

However there are several problems with this approach. Moving masses of this magnitude to a position almost halfway along the radius of the sail would be a considerable engineering challenge as motors would have to quickly and accurately reposition the masses. This is unlikely given the magnitude of the masses and the distances involved. Therefore there would likely be considerable delay in achieving the desired position of the masses and hence the required torques. In addition the control torques are dependent on the attitude of the sail and the position of the sail on the orbit, meaning that the value of F_{SRP_x} will not be constant and so the maximum torques available will vary. If the torques cannot be produced when required, tracking references may be unfeasible. Furthermore, the moments of inertia of the spacecraft will change as the large masses move, altering the symmetry and perhaps rendering the references invalid.

The control torques which are required to track the references could be reduced in a number of ways. These include adding an extra term in the cost function during the parametric optimisation which minimises the control torques, as in [22]. In addition the control torques could be reduced by increasing manoeuvre time which would further decrease the body rates. However this may cause unacceptable drift from the target orbit during the reorientation. Finally conventional thrusters could be used to produce the required large control torques, without significant delay, but as stated above the impulsive nature of the torques could excite the sail structure. It will be necessary to implement a realistic actuation method, including actuator dynamics, in order to assess the feasibility and practicality of the method.

Figures 3 and 6 show the deviation from the reference tracks throughout the manoeuvres. While these values are small, they are still significant. The accuracy of the method would improve if the attitude of the spacecraft in the non-spinning frame could be accurately controlled. At the moment at the end of the manoeuvre the spacecraft is simply brought to a state of pure spin, leading to a drift from the desired attitude. A solution to this may be to find the quaternion differential equations which describe the attitude of the non-spinning frame with respect to the orbit frame, and describe the kinematics of the spacecraft in this way. This would then allow a quaternion component to be included in the control that brings the spacecraft to a state of pure spin, correcting any error in position.

Finally, in order to truly assess the benefits of the method a structural analysis of the spacecraft during the manoeuvre must be carried out. The bending modes of the spacecraft could be found and then compared against the control frequency to ensure that the spacecraft structure is not excited, while the bending equations could be integrated alongside the Euler equations to assess whether the motion planning method can be used in the face of the errors introduced by a flexing spacecraft.

VII. CONCLUSIONS

This paper has applied a method for generating attitude reference motions to a $70m$ radius spin-stabilised disk sail in a heliocentric orbit. The kinematics of the spinning sail were written in terms of the Lie algebra on $SU(2)$ and the optimal Hamiltonian found through application of Pontryagin's maximum principle. The optimal angular velocities and time evolution of the quaternions were found using Lax Pair integration, enabling the completely analytical expressions to be parametrically optimised to produce reference tracks for a given set of boundary conditions.

The method was tested in simulation during two re-pointing manoeuvres related to an inclination change orbital manoeuvre. It was found that while the references enabled the spinning sail to reach a desired attitude while minimising the body rates, the control torques required were beyond the current technological limits of sliding ballast or electrochromic control. In addition, the need to bring the sail to a state of pure spin at the end of the manoeuvre resulted in a small error in the final pointing direction.

Future work will see a method implemented to minimise control torques during the parametric optimisation, and a sliding mass method modelled to assess whether the desired control torques can be feasibly produced. In addition a structural analysis will be carried out to determine whether the minimisation of the body rates reduces the impact of the attitude manoeuvre on the sail structure, justifying the increased control torques that maintaining spin stabilisation throughout requires.

References

- [1] Macdonald, M. and McInnes, C.R., "GeoSail; An enhanced magnetosphere mission, using a small low cost solar sail", In: Proceedings of the 51st International Astronautical Congress, Rio de Janeiro, Brazil, October 2000.
- [2] Macdonald, M., Hughes, G.W., McInnes, C.R., Lyngvi, A., Falkner, P. and Atzei, A., "GeoSail: an elegant solar sail demonstration mission", *Journal Spacecraft and Rockets* 44 (4), pp. 784-796, 2007a.
- [3] Macdonald, M., Hughes, G.W., McInnes, C.R., Lyngvi, A., Falkner, P. and Atzei, A., "Solar polar orbiter: a solar sail technology reference study", *Journal of Spacecraft and Rockets* 43 (5), 960-972, 2006.
- [4] Macdonald, M., McInnes, C.R. and Hughes, G.W., "Technology requirements of exploration beyond Neptune by solar sail propulsion", *Journal of Spacecraft and Rockets* 47 (3), 472-483, 2010.
- [5] Wie, B., "Solar sail attitude control and dynamics: part 1", *Journal of Guidance, Control and Dynamics*, 27(4), pp. 526-535.

- [6] Polites, M., Kalmanson, J. and Mangus, D., "Solar sail attitude control using small reaction wheels and magnetic torquers", Proceedings of the Institution Of Mechanical Engineers Part G - Journal Of Aerospace Engineering, 222(G1), pp.53-62, 2008.
- [7] Wie, B., "Space Vehicle Dynamics and Control," AIAA Education Series, 2nd addition, 2008.
- [8] Wie, B., Murphy, D., "Solar-sail attitude control design for a sail flight validation mission", Journal of Spacecraft and Rockets, 44 (4), pp. 809-821, 2007.
- [9] Bolle, A., Circi, C., "Solar sail attitude control through in-plane moving masses", Journal of Aerospace Engineering, 222 (1), pp. 81-94, 2008.
- [10] Scholz, C., Romagnoli, D., Dachwald, B. and Theil, S., "Performance analysis of an attitude control system for solar sails using sliding masses", Advances in Space Research, 48, pp. 1822-1835, 2011.
- [11] Romagnoli, D. and Oehlschlagel, T., "High performance two degrees of freedom attitude control for solar sails", Advances in Space Research, 48, pp. 1869-1879, 2011.
- [12] Steyn, W.H. and Lappas, V., "Cubesat solar sail 3-axis stabilization using panel translation and magnetic torquing", Aerospace Science and Technology, 15, pp. 476-485, 2011.
- [13] McInnes, C.R., "Solar Sailing: Technology Dynamics and Mission Applications", Springer-Praxis, Chichester, 1999.
- [14] Funase, R., Shirasawa, Y., Mimasu, Y., Mori, O., Tsuda, Y., Saiki, T. and Kawaguchi, J., "On-orbit verification of fuel-free attitude control system for spinning solar sail utilizing solar radiation pressure", Advances in Space Research, 48, pp. 1740-1746, 2011.
- [15] Sidi, M.J., "Spacecraft Dynamics and Control: A practical engineering approach", Cambridge University Press, 2002.
- [16] Scrivener, S.L. and Thompson, R.C., "Survey of Time-Optimal attitude Maneuvers", Journal of Guidance, Control, and Dynamics, 17(2), pp. 225-231, 1994.
- [17] Vadali, S.R. and Junkins, J.L., "Optimal open loop and stable feedback control of rigid spacecraft attitude maneuvers", Journal of Astronautical Sciences, 32(2), pp. 105-122, 1984.
- [18] Tsiotras, P., "Stabilization and Optimality Results for the Attitude Control Problem", Journal of Guidance Control and Dynamics, 19(4), 1996.
- [19] Bilimoria, K.D., Wie, B., "Time-optimal three-axis reorientation of a rigid spacecraft", Journal of Guidance, Control, and Dynamics, 16(3), pp. 446-452, 1993.
- [20] Seywald, H., Kumar, R.R., Deshpande, S.S. and Heck, M.L., "Minimum fuel spacecraft reorientation", Journal of Guidance, Control, and Dynamics, 17(1), pp. 21-29, 1994.
- [21] Lawton, J., Beard, R. and McLain, T., "Successive Galerkin approximation of nonlinear optimal attitude control", Proceedings of the American Control Conference, San Diego, California, June, 1999.
- [22] Biggs, J. and Horri, N., "Optimal geometric motion planning for spin-stabilized spacecraft", Systems and Control Letters, 61 (4), pp. 609-616, 2012.
- [23] Bate, R.R., Mueller, D.D. and White, J., "Fundamentals of Astrodynamics," Dover Books, pp. 13, pp. pp. 156-159, 1971.
- [24] Jurdjevic, V., "Geometric Control Theory", Advanced Studies in Mathematics, Cambridge University Press, 52, 1997.